JOURNAL OF VIROLOGY, Feb. 2001, p. 1387–1400 Vol. 75, No. 3
0022-538X/01/$04.00+0 DOI: 10.1128/JVI.75.3.1387–1400.2001

Adenovirus Serotype 7 Retention in a Late Endosomal Compartment prior to Cytosol Escape Is Modulated by Fiber Protein

NAOKI MIYAZAWA,[1] RONALD G. CRYSTAL,[1,2] AND PHILIP L. LEOPOLD[1]*

Division of Pulmonary and Critical Care Medicine[1] and Institute of Genetic Medicine,[2] Weill Medical College of Cornell University, New York, New York

Received 26 June 2000/Accepted 19 October 2000

The intracellular trafficking of adenovirus (Ad) subgroup B (e.g., Ad7) differs from that of subgroup C (e.g., Ad5) in that Ad5 rapidly escapes from endocytic compartments following infection whereas Ad7 accumulates in organelles. To assess the hypothesis that Ad7 is targeted to the lysosomal pathway, Ad7 and Ad5 were conjugated with fluorophores and their trafficking in A549 epithelial cells was analyzed by fluorescence microscopy. Within 1 h after infection, Ad7, but not Ad5, accumulated in the cytoplasm of A549 cells. The pH in the environment of Ad5 was nearly neutral (pH 7), while Ad7 occupied acidic compartments (pH 5) over the first 2 h with a gradual shift toward neutrality by 8 h. Ad7 partially colocalized with α_2-macroglobulin and late endosomal and lysosomal marker proteins, including Rab7, mannose-6-phosphate receptor, and LAMP-1. The pH optimum for membrane lysis by Ad7, as well as a chimeric Ad5 capsid that expressed the Ad7 fiber (Ad5fiber7), was pH 5.5, while that for lysis by Ad5 was pH 6.0. Thus, the native trafficking pathway for Ad7 involves residence in late endosomes and lysosomes, with information encoded in the Ad7 fiber acting as a pH-dependent trigger for membrane lysis and escape to the cytosol.

Many of the 49 human adenovirus (Ad) serotypes have distinct pathophysiology, suggesting underlying variations in the biological life cycle of the viruses (21, 45). The differences can partially be explained in terms of different tropisms secondary to differences in high- and low-affinity receptors utilized by the different adenovirus serotypes (11, 30, 39, 48), but the differences are likely to extend beyond the plasma membrane and may encompass the intracellular trafficking characteristics of the serotypes.

Entry into and trafficking through target cells has been most throughly studied using subgroup C viruses. Binding to target cells occurs via a high-affinity interaction between the fiber protein and the coxsackievirus-Ad receptor on the cell surface (3, 52). Subgroup C Ad then rapidly enter cells by endocytosis through interaction of the penton base protein of Ad with vitronectin binding integrins on the cell surface, including $\alpha_v\beta_3$, $\alpha_v\beta_5$, $\alpha_M\beta_2$, and $\alpha_5\beta_1$ integrins (2, 10, 22, 56, 57). Endosomal membranes are lysed by adenovirus, allowing the escape of capsids to the cytosol (4, 15, 18, 26, 38, 43, 44, 56). Then adenovirus translocates to the nucleus by using microtubules in cytoplasm, binds to the nuclear envelope, and inserts its genome through nuclear pore complexes (5, 6, 8, 19, 26, 27, 34, 42, 49, 58).

The most striking differences in intracellular trafficking among serotypes has been observed in comparisons of the infection pathways of Ad subgroups B and C. Although the high-affinity receptor of subgroup B differs from that of subgroup C (11, 48), both serotype 5 (Ad5) and Ad7 enter the cell with similar kinetics (33). The major distinctions in the trafficking of Ad5 and Ad7 relate to the observation that Ad7 is found in membranous organelles for hours after infection whereas subgroup C viruses escape rapidly to the cytosol (5, 8). Subgroup B and C viruses also have different characteristics of endocytic trafficking. Subgroup B Ad remain colocalized with cointernalized markers for a longer period than do subgroup C Ad (33). Conversely, subgroup C viruses induce a more rapid release of cointernalized particles to the cytoplasm than do subgroup B viruses (11). Finally, subgroup C Ad can be found associated with the nuclear envelope rapidly following infection while subgroup B Ad exhibit a slower association with the nucleus (6, 33). This observation correlates with the observation that capsids of subgroup B Ad maintain association with their genomes for a longer period following infection than do those of subgroup C Ad (33).

The key difference in the intracellular trafficking of the two Ad subgroups appears to be the length of time that virions are retained within membranous organelles before escaping to the cytosol. In general, materials that enter cells via endocytosis can follow one of two major routes: (i) the endocytic recycling pathway, in which membrane proteins and membrane-bound proteins are collected in a tubulovesicular compartment, termed the endocytic recycling compartment, prior to trafficking back to the cell surface; or (ii) the lysosomal pathway, in which a select set of membrane proteins, ligands that have dissociated from their receptors, and soluble materials occupy a compartment termed the sorting endosome, which later matures and acidifies to become a late endosome and finally a lysosome (36).

Based on previously published ultrastructural studies suggesting aggregation of Ad7 in an endocytic compartment (6, 8) and cosedimentation with lysosomal enzymes (6, 37), we hypothesized that the subgroup B virus Ad7 follows the lysosomal trafficking pathway after endocytosis. To follow the intra-

* Corresponding author. Mailing address: Institute of Genetic Medicine, Weill Medical College of Cornell University, 520 E. 70th St., ST 505, New York, NY 10021. Phone: (212) 746-2258. Fax: (212) 746-8383. E-mail: geneticmedicine@med.cornell.edu.

cellular fate of subgroup B Ad, we used a series of functional analyses of intracellular compartments of cells infected with Ad5 (subgroup C) and Ad7 (subgroup B), including evaluation of the pH, characterization of lysosomally targeted endocytic ligands, and localization of organelle marker proteins. Finally, we tested the hypothesis that Ad7 trafficked to lysosomes prior to escape to the cytosol by evaluating the pH optimum of membrane lysis by Ad7. The results suggested that Ad7, but not Ad5, trafficked in the lysosomal pathway following endocytosis and that this route favored the escape of Ad7 to the cytosol by delivering Ad7 to a low-pH compartment.

MATERIALS AND METHODS

Cells. The A549 human lung epithelial cell line (CCL-185; American Type Culture Collection, Manassas, Va.) and the KB human epithelial cell line (CCL-17; American Type Culture Collection) were cultured in Dulbecco's modified Eagle's medium supplemented with 10% fetal bovine serum, 50 U of penicillin per ml, and 50 μg of streptomycin (GIBCO/BRL Life Technologies, Inc., Gaithersburg, Md.) per ml. For microscopy experiments, the cells were seeded in 35-mm coverslip dishes and cultured to approximately 50% confluence. The 7-mm-diameter well in each coverslip dish contained 10^4 cells. For other experiments, cells were plated as described below.

Ad vectors. The Ad used in this study were recombinant, $E1^-$, $E3^-$ replication-deficient viruses containing a cytomegalovirus early/intermediate promoter-enhancer driving expression of the chloramphenicol acetyltransferase gene in the E1 position (23). The identical expression cassette was inserted into a viral backbone encoding either an Ad subgroup B, Ad7 vector or an Ad subgroup C, Ad5 vector (1, 23). Ad5fiber7 is a chimeric vector composed of an Ad5 capsid with an Ad7 fiber replacing the Ad5 fiber protein (16). Ad vectors were propagated in the 293 human embryonic kidney cell line, purified, and stored at −70°C, as previously described (40, 41).

Quantitative analysis of Ad genome delivery. To evaluate delivery of the Ad genomic DNA to the nucleus over time, Ad DNA and β-actin DNA of A549 cells were analyzed using quantitative real-time PCR (TaqMan PCR detection; Perkin-Elmer, Applied Biosystems Division, Foster City, Calif.) as previously described (33). Briefly, A549 cells (2×10^6) cultured in a 10-cm culture plate were infected with Ad5 or Ad7 (2×10^9 particles/ml, 10^3 particles/cell) at 37°C for 10 min, washed to remove unbound Ad, and incubated for 0 to 8 h at 37°C. At each time point, the cells were collected and half of the cells were used for extraction of total cellular DNA using the QIAamp blood kit (Qiagen Inc., Santa Clarita, Calif.). The remaining cells were used for nuclear isolation as previously described (33, 35). For Ad7 analysis, a fluorogenic probe (carboxyfluorescein-TC CCGTGATGGGCAGGCAGAC-carboxytetramethylrhodamine) was designed to anneal to the target between the sense primer (GGATGATGCTGATCCCC ATT) and the antisense primer (TCGGGTCACTGATGGTAGCC) in the Ad7 genome. A similar set of probes was used for analysis of the Ad5 E2 region and β-actin gene of A549 cells as previously described (33). Samples were amplified for 40 cycles in a Perkin-Elmer 7700 sequence detection system with continuous monitoring of the fluorescence. Data were processed by the SDS 1.6 software package (Perkin-Elmer). To control for differences in DNA recovery from samples, the data are presented as a ratio of Ad genome DNA to cellular β-actin DNA.

Conjugation of fluorescent dyes with Ad. Ad vectors were conjugated with Cy3 fluorescent dye (Amersham Life Science, Arlington Heights, Ill.) or 5- and 6-carboxyfluorescein succinimidyl ester (Molecular Probes, Eugene, Oreg.) to allow assessment by fluorescence microscopy as previously described (26, 33). Cy3-Ad and carboxyfluorescein-Ad stocks were maintained in 30% glycerol–50 mM Tris-HCl (pH 7.8)–150 mM $NaCl_2$–10 mM $MgCl_2$ at −20°C. The amount of dye incorporated into Cy3-Ad and carboxyfluorescein-Ad was measured by recording the absorbance at 552 and 495 nm, respectively, using a spectrophotometer (no. Du640; Beckman, Fullerton, Calif.). For preparations used in this study the dye-to-capsomere ratio ranged from 0.3 to 1.9. We previously reported that conjugation of vectors with fluorophore resulting in comparable dye-to-capsomere ratios did not change the titer of vectors within the experimental error of the titer determination assay (26).

Fluorescence microscopy. Fixed samples were observed using a Nikon Microphot SA microscope equipped with a 100× or 60× PlanApo objective lens. Live cells were viewed on a Nikon Diaphot inverted microscope equipped with a 100× N.A. 1.25 objective, Nikon NP2, thermostatic heater, stage incubator, and electronic filter wheel with 450- and 490-nm excitation filters. Images were collected and analyzed using a cooled charge-coupled device camera (Princeton Instruments, Trenton, N.J.) and Metamorph imaging software (Universal Imaging, West Chester, Pa.) as previously described (26). For quantitative studies, five fields per condition were acquired and used for digital image analysis. Following background substraction, the fluorescence intensities over 1% of the dynamic range of the camera were collected and digitally analyzed.

Virus accumulation in cytoplasm. To compare the size and distribution of local viral accumulations of Cy3-Ad5 and Cy3-Ad7 in cytoplasm, A549 cells in coverslip dishes (10^4 cells in the coverslip well) were rinsed three times with binding buffer (modified Eagle's medium supplemented with 1% bovine serum albumin and 10 mM HEPES) (pH 7.3) and infected (pulse) with Cy3-Ad (10^{11} particles/ml; 30-μl volume added to the coverslip well) for 10 min at 37°C, giving a viral concentration of 3×10^5 particles per cell. Ad vectors with identical dye-to-capsomere ratios (0.3) were used. After infection, the cells were washed three times with phosphate-buffered saline (pH 7.4) (PBS) and fixed with 4% paraformaldehyde (at 23°C for 15 min) or washed three times with binding buffer to wash out unbound virus and incubated (chase) for 30 min at 37°C prior to fixation. Following fluorescence microscopy with digital image acquisition, the corresponding fluorescent signal from Cy3 virions was measured using a pixel area algorithm in the image analysis software. Pixel size calibration was performed using InSpeck microscopic size standards (Molecular Probes). A 2.5-μm particle had a diameter of 25 ± 0.6 pixels ($n = 10$); i.e., each pixel corresponded to an area of 100 nm by 100 nm.

Intracellular pH measurement. To determine the intracellular pH, carboxyfluorescein-Ad5 or Ad7 was used as previously described (27). Briefly, following infection with carboxyfluorescein-Ad as described for Cy3-Ad infection (see above), optical fields containing live cells maintained at 37°C in Leibowitz's L-15 medium (Life Technologies) were imaged using either 450-or 490-nm excitation wavelengths. The ratio of fluorescence intensities (I_{490}/I_{450}) correlates with the pH in the environment of the fluorophore. Fluorescence ratios were interpreted by comparison with standard curves generated by incubating Ad-infected cells in buffers containing 50 mM methylamine in Leibovitz's L-15 medium adjusted to various pH values (pH 5.0 to 7.5) (31, 32). More than 500 individual spots in five different fields were analyzed for each condition.

Coincubation of Ad with α_2M. Cy3-conjugated α_2-macroglobulin (Cy3-α_2M; kindly provided by F. R. Maxfield, Weill Medical College of Cornell University) was used as a marker to label endocytic trafficking compartments including late endosomes to lysosomes (36). To demonstrate specific endocytic trafficking of α_2M in A549 cells, cells were incubated with Cy3-α_2M (10 μg/ml) and a marker for the endocytic recycling pathway, fluorescein-5-isothiocyanate-conjugated transferrin (59) (FITC-Tf; kindly provided by F. R. Maxfield)(10 μg/ml), for 15 min at 37°C, washed three times in binding buffer, and then incubated for 0 or 45 min in binding buffer at 37°C.

Colocalization of Ad7 and α_2M was investigated by infecting A549 cells for 10 min at 37°C with carboxyfluorescein-Ad7 (10^{11} particles/ml; 3×10^5 particles/cell), washing them three times in binding buffer, and incubating them in Cy3-α_2M (10 μg/ml) for 15 min. After three washes with binding buffer, the cells were incubated for 0, 45, or 105 min at 37°C, corresponding to total infection times of 15, 60, and 120 min, respectively. The cells were washed, fixed, stained with 4′, 6-diamidino-2-phenylindole (DAPI) and observed by fluorescence microscopy.

Colocalization of Ad with endosomal proteins. To identify endosomal compartments containing Ad7, indirect immunofluorescence experiments were conducted on cells infected with carboxyfluorescein-Ad7 using primary antibodies to several endosome-associated proteins. A549 cells were infected with carboxyfluorescein-Ad7 (10^{11} particles/ml; 3×10^5 particles/cell) at 37°C for 10 min, washed three times with binding buffer, and incubated for the indicated times. The cells were washed three times in PBS, fixed with 4% paraformaldehyde for 15 min, and permeabilized with ice-cold 100% methanol for 20 min. The cells were washed and blocked with normal serum (10% [vol/vol] in PBS) for 20 min at 23°C. Monolayers were incubated for 60 min with primary antibodies diluted in 1.5% serum (Calbiochem, San Diego, Calif.) matched to the species of the secondary antibody, washed, and incubated at 23°C for 60 min with species-matched fluorophore-conjugated secondary antibodies. The primary antibodies used were monoclonal mouse anti-transferrin receptor (clone B3/25; Boehringer Mannheim, Indianapolis, Ind.), mouse anti-lysosome-associated membrane protein 1 (clone H4A3; Pharmingen, San Diego, Calif.), polyclonal rabbit anti-mannose-6-phosphate receptor (kindly provided by L. Traub, Washington University), polyclonal rabbit anti-Rab 4, rabbit anti-Rab 5, goat anti-Rab 7, and goat anti-Rab 11 (Santa Cruz Biotechnology, Santa Cruz, Calif.). The secondary antibodies used were Texas red-conjugated goat anti-rabbit immunoglobulin G (Calbiochem), donkey anti-goat immunoglobulin G (Jackson ImmunoResearch Lab., West Grove, Pa.), and goat anti-mouse IgG (Molecular Probes).

Quantitative comparison of the Ad5 and Ad7 motility. Cy3-Ad translocation in living A549 cells was quantified as described previously (27). A549 cells were infected with Cy3-Ad5 or Cy3-Ad7 (10^{11} particles/ml; 3×10^5 particles/cell) for 10 min at 37°C, washed, and incubated in binding buffer at 37°C as described above. The cells were washed three times with Liebowitz L-15 medium and transferred to a Nikon Diaphot inverted microscope equipped as described above. Ten successive images of a single microscopic field were acquired at 1-s intervals. Ad translocation was quantified by determining the number of linear translocations ("linear translocation" defined as >2 μm of uninterrupted movement), the number of virus particles in the field, and the duration of observation. To ensure equal weighing of each segment, data are presented as the number of translocations per virion per minute of observation.

Ad-induced cell membrane lysis assay. Ad-induced cell membrane lysis was assayed by measuring [^{3}H]choline release (44, 56). KB cells were plated at a density of 2×10^4cells/well in a 96-well plate and used 24 h later. The cells were washed once with Dulbecco's modified Eagle's medium containing 0.2% BSA and labeled with 5 μCi of [^{3}H]choline per ml (1 mCi/ml; NEN Life Science Products, Boston, Mass.) in the medium at 37°C for 1 h. The cells were then washed once with ice-cold HEPES-buffered saline (5 mM HEPES [pH 7.0], 0.9% NaCl, 0.2% BSA, 1 mM $CaCl_2$, 1 mM $MgCl_2$, 50 mM NaN_3) and incubated at 4°C for 1 h with Ad5, Ad7, or Ad5fiber7 (10^{11} particles/well; 5×10^6 particles/cell). After virus binding, the cell samples were washed once with permeability buffer, prepared by titrating morpholineethanesulfonic acid (MES)-buffered saline (100 mM MES [pH 5.0] containing 0.9% NaCl, 0.2% BSA, 1 mM $CaCl_2$, 1 mM $MgCl_2$, and 50 mM NaN_3) with HEPES-buffered saline (100 mM HEPES [pH 7.5] with the same supplements) to achieve the desired pH. The cells were incubated at 37°C for 1 h. After incubation, the permeability buffer was collected to determine ^{3}H release, while cell-associated ^{3}H was determined by incubating the cells with 0.1 N NaOH at 37°C for 1 h. The percent [^{3}H]choline release was calculated by measuring the counts released into the permeability buffer and the counts that remained cell associated using a liquid scintillation counter.

Statistical Evaluation All data are presented as means ± standard errors of the means. Statistical evaluations were carried out by using the two-tailed Student *t* test.

RESULTS

Kinetics of Ad DNA delivery to the nucleus. To examine the rate of DNA transfer to the nucleus, real-time quantitative PCR (TaqMan PCR) was performed using primers specific for the Ad5 genome or the Ad7 genome. Both the Ad5 and Ad7 genomes were stable in cells throughout the time course of the experiment (Fig. 1A). The difference in the amount of the Ad5 genome found in total-cell lysate 1 h after infection ($1.31 \times 10^{-2} \pm 0.04 \times 10^{-2}$Ad/β-actin gene) versus 8 h after infection ($1.58 \times 10^{-2} \pm 0.02 \times 10^{-2}$ Ad/β-actin gene) was not significant ($P > 0.25$). Similarly, the difference in the amount of Ad7 genome found in total-cell lysate 1 h after infection ($2.05 \times 10^{-2} \pm 0.02 \times 10^{-2}$ Ad/β-actin gene) versus 8 h after infection ($2.44 \times 10^{-2} \pm 0.04 \times 10^{-2}$ Ad/β-actin gene) was not significant ($P > 0.25$). Ad7 genome accumulation in the nucleus, measured as percentage of total-cell-associated viral DNA, was slower than Ad5 accumulation with the two vectors exhibiting half times of DNA transfer to nuclei of 220 and 40 min, respectively (Fig. 1B).

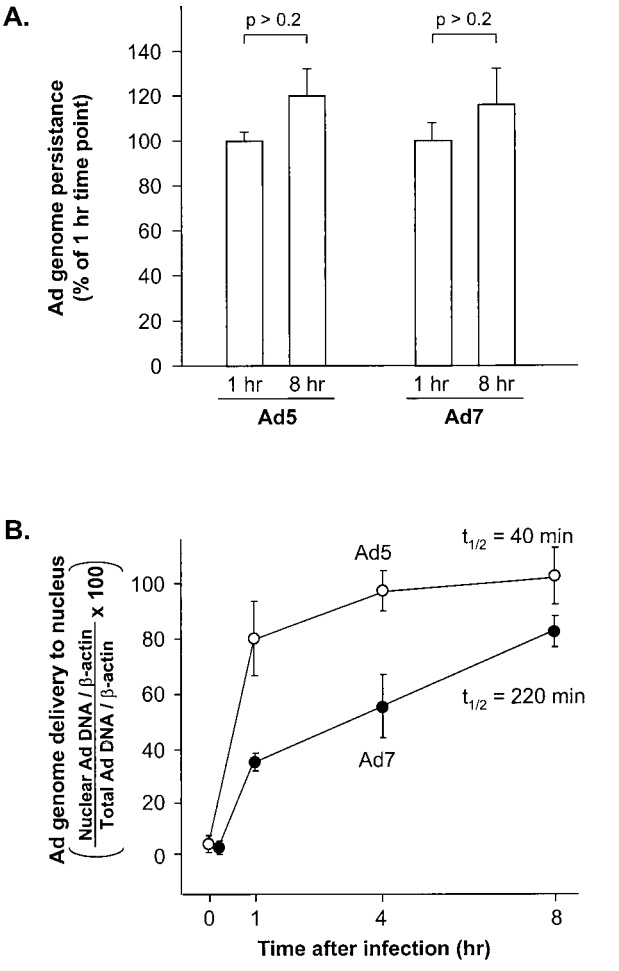

FIG. 1. Quantitative evaluation of Ad5 and Ad7 genome persistence in cells and delivery of the genome to the nucleus at various times after a 10-min infection. A549 cells were infected with Ad5 or Ad7 (10^3 particles/cell) at 37°C for 10 min. The cells were washed and incubated for 0 to 8 h at 37°C. They were then harvested, and DNA was extracted from the total-cell lysate or from isolated nuclei. Ad DNA was quantified by a fluorogenic PCR assay using probes for Ad5 or Ad7 and compared to an internal standard (cellular β-actin gene). (A). Ad DNA persistence in A549 cells. The amounts of Ad5 and Ad7 DNA in A549 cells were compared at 1 and 8 h after infection. Data are presented as a percentage of the DNA content at 1 h (B). Percentage of the Ad genome delivered to the nucleus. The data are presented as the ratio of nuclear Ad genome copies (normalized to nuclear β-actin gene copies) to total-cell lysate Ad genome copies (normalized to lysate β-actin gene copies). Shown are the analyses for Ad5 and Ad7. The data are presented as the mean ± standard error of three experiments.

Local intracellular accumulation of Ad7. Prior analyses demonstrated that Ad7 capsids accumulated in an intracellular compartment whereas Ad5 capsids remained dispersed (6, 8, 33). The fate of Ad5 and Ad7 in the cytoplasm of A549 cells was investigated by infecting A549 cells with virions fluorescently conjugated to the fluorophore Cy3 (Cy3-Ad5 or Cy3-Ad7). Immediately after infection, the sizes of fluorescent spots were comparable for the two viruses (Fig. 2A, B). Cy3-Ad morphology was analyzed again 30 min following infection, a time point deliberately chosen prior to Ad5 accumulation at the nuclear envelope to enable analysis of cells that still had a significant number of Ad5 virions that could be resolved in the cytoplasm. When cells were incubated for 30 min following infection, the size distribution of Cy3-Ad5 spots was unchanged (Fig. 2C) while the size distribution of fluorescent spots in Cy3-Ad7-infected cells shifted toward larger and brighter signals (Fig. 2D). A quantitative analysis of spot size demonstrated the shift toward vector accumulation for Ad7 but not Ad5 (Fig. 2E and F). The results demonstrate localized accumulation of Ad7, but not Ad5, in the cytoplasm. Similar to

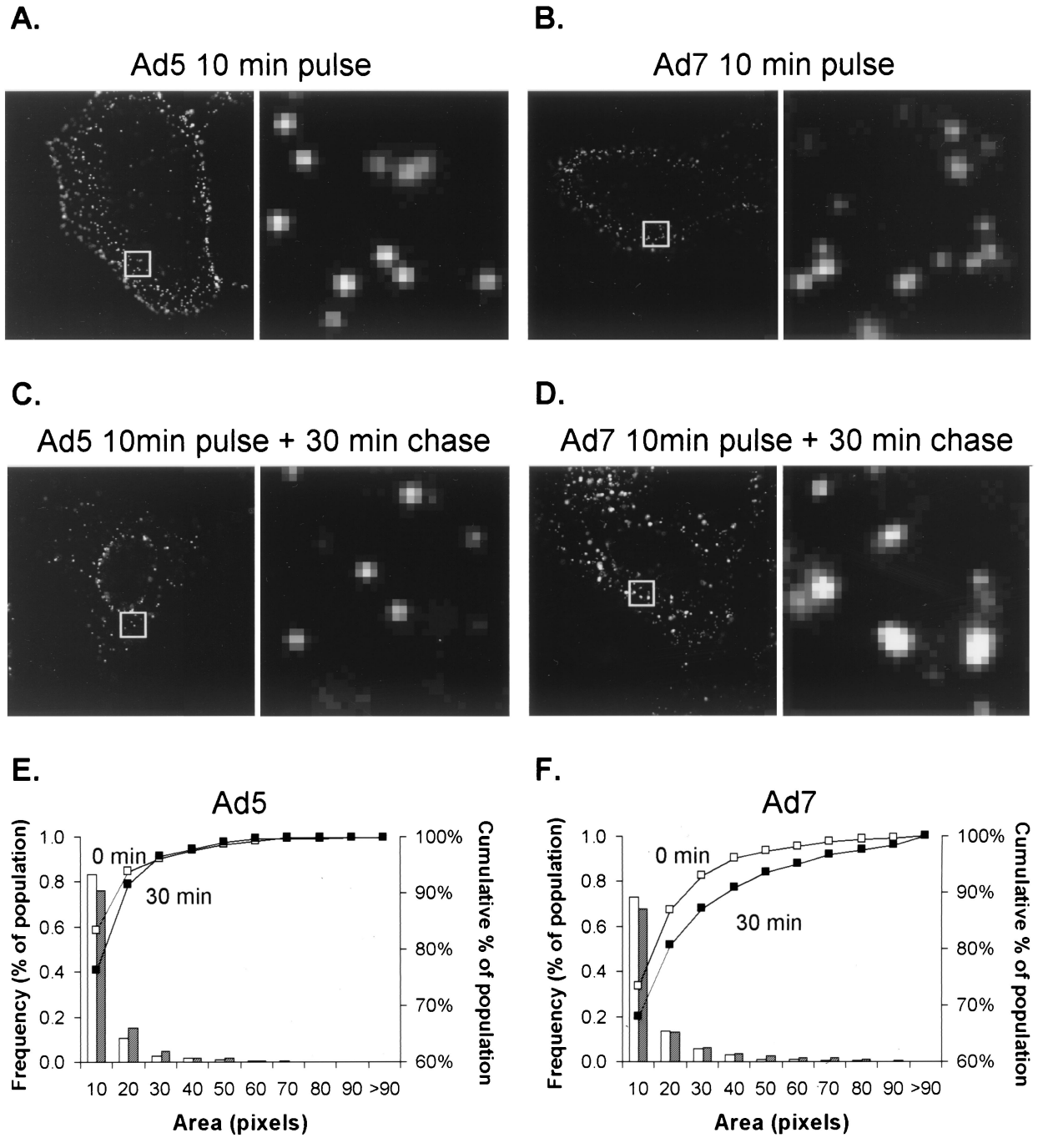

FIG. 2. Localized intracellular accumulation of Ad7 compared to Ad5. A549 cells were incubated with Cy3-Ad (10^{11} particles/ml) for 10 min at 37°C, washed, and immediately fixed (10-min pulse) or incubated for 30 min at 37°C prior to fixation (10-min pulse plus 30-min chase). (A to D) Images of Cy3-Ad5 and Ad7. For each pair of panels, the right panels are ×8 magnifications of the box in the left panel; the ×8 magnification provides an overview of the regions and extent of localized accumulation of the fluorophore-labeled virus. (E) Histogram of the frequency of Cy3-Ad5 as a function of the pixel number. Open bars and open squares (□) represent a 10-min pulse, whereas shaded bars and solid squares (■) represent a 10-min pulse followed by a 30-min chase (F) Histogram of the frequency of Cy3-Ad7 as a function of pixel number. The cumulative percentage curve of Ad7 (■) was shifted toward the right at 30 min, indicating an increase in the mean pixel area of the fluorescent spots as infection progressed. The dimensions of each box analyzed are 3.5 by 3.5 μm.

A549 cells, KB cells showed localized accumulation of Ad7 but not Ad5 in the cytoplasm (data not shown).

Determination of the pH of Ad-containing compartments. Fluorophore-Ad conjugates can be used to evaluate the pH in the immediate environment of the virus in living cells if the fluorophore has pH-sensitive optical properties (13, 32). To measure the pH in the immediate environment of Ad5 and Ad7, the capsids were conjugated with the pH-sensitive dye

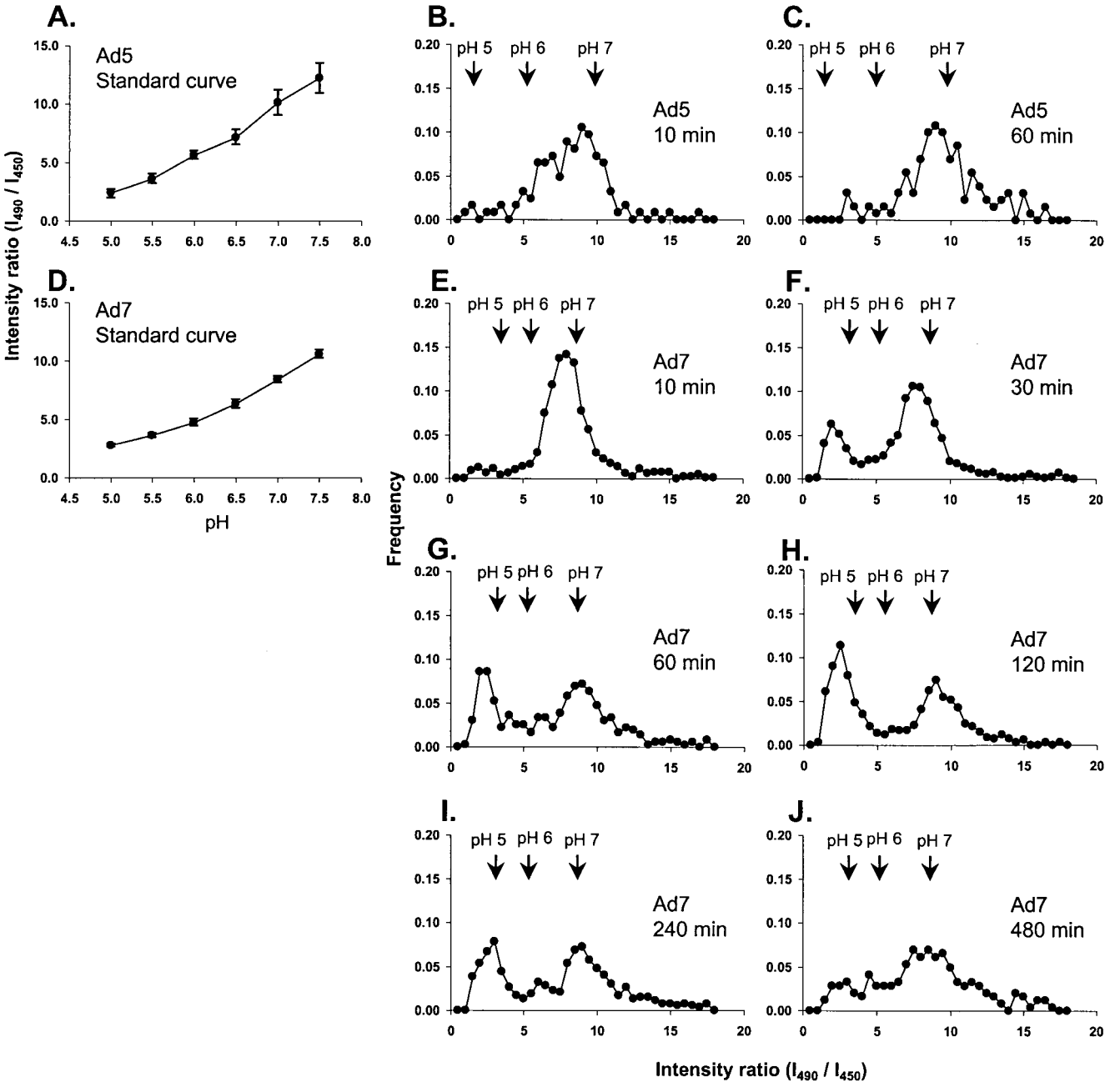

FIG. 3. Comparison of the pH of compartments containing Ad5 or Ad7. A549 cells were infected with carboxyfluorescein-Ad (10^{11} particles/ml) for 10 min at 37°C and incubated at 37°C for various times. pH measurements were performed in living cells by recording carboxyfluorescein emission intensity following excitation at either 490 or 450 nm. (A). Standard curve of carboxyfluorescein-Ad5 using cells equilibrated with 50 mM methylamine buffers (pH 5.0 to 7.5). The fluorescence intensity ratio (I_{490}/I_{450}) is related to the pH of the standard medium. Bars show the 95% confidence interval. (B) Carboxyfluorescein-Ad5, 10-min pulse (infection) and 10-min chase (incubation). (C) Carboxyfluorescein-Ad5, 10-min pulse and 60-min chase. (D) Standard curve of carboxyfluorescein-Ad7. (E to J) Carboxyfluorescein-Ad7, 10-min pulse with various chase times as indicated (10 to 480 min).

carboxyfluorescein (51). In living cells, the intensity of fluorescence emission was determined using a pH-sensitive excitation wavelength (490 nm) and a pH-insensitive excitation wavelength (450 nm) (Fig. 3). The ratio of emission intensities resulting from the two excitation (I_{490}/I_{450}) wavelengths corresponded to the intracellular pH, demonstrated through the use of control buffer solutions (Fig. 3A and D). The earliest time point observed, 10 min following removal of unbound virions from the medium, corresponded to the time at which 100% of virions are intracellular (33). After a 10-min chase, the Ad5 ratios were distributed between pH 6.0 and 7.0, indicating that Ad5 was within early endosomes or free in cytosol (Fig. 3B).

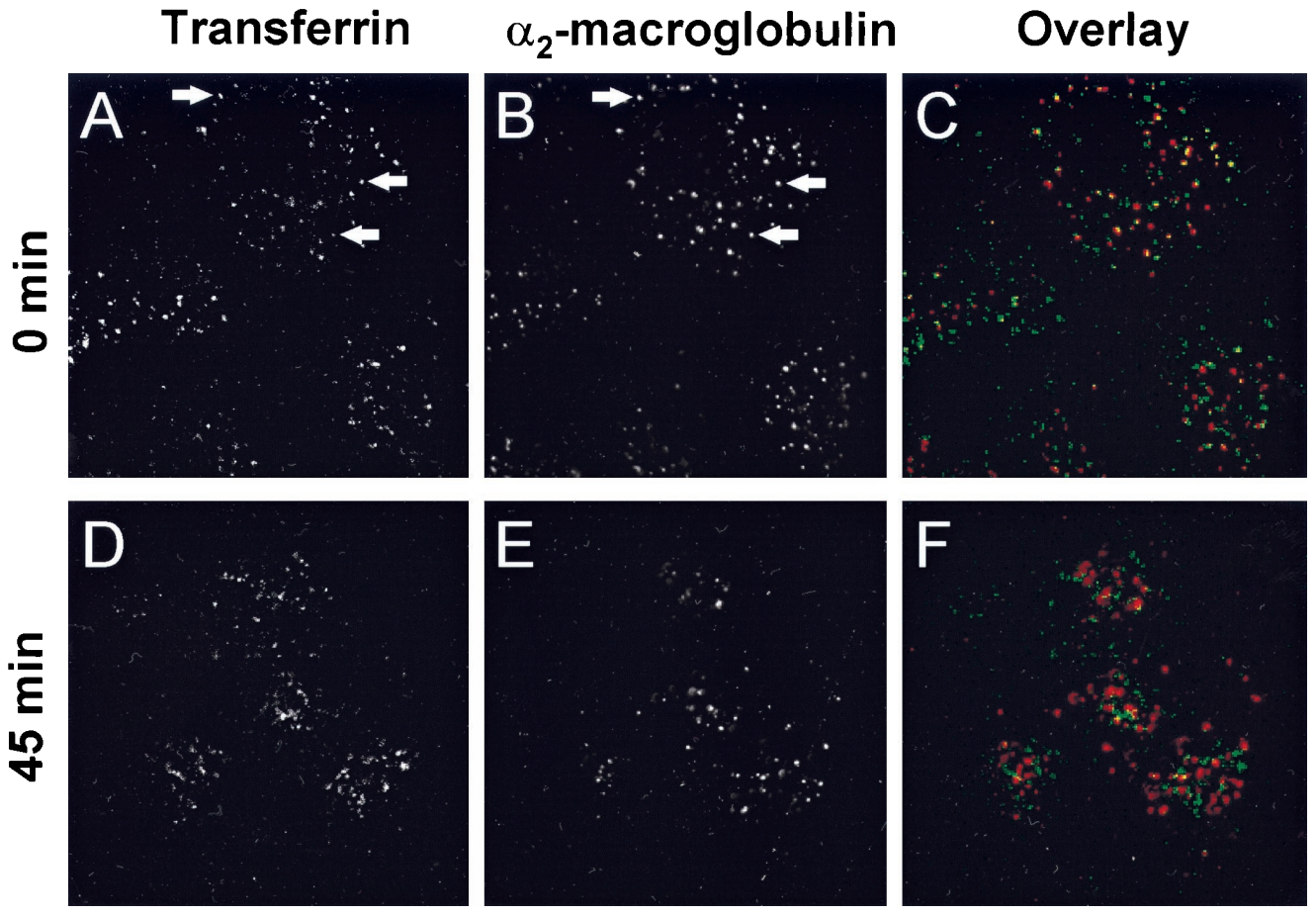

FIG. 4. Endocytic trafficking in A549 cells. The cells were labeled with Cy3-α_2M (10 μg/ml) and FITC-Tf (10 μg/ml) for 15 min, washed, and incubated for 0 or 45 min. The left column shows FITC-Tf; the center column shows Cy3-α_2M; and the right column shows a color overlay of the signals (FITC-Tf, green; Cy3-α_2M, red; colocalization, yellow). (A) FITC-Tf, without incubation. (B) Cy3-α_2M, without incubation. (C) Overlay of panels A and B (D) FITC-Tf, 45-min incubation. (E) Cy3-α_2M, 45-min incubation. (F) Overlay of panels D and E. Arrows indicate examples of colocalization of Cy3-α_2M and FITC-Tf. Field width, 50 μm.

After a 60-min chase, the peak of the Ad5 pH distribution was shifted toward neutrality (Fig. 3C), indicating that most of the Ad5 virions had escaped from acidic organelles to the neutral cytosol in A549 cells within 1 h.

At 10 min after infection, the pH distribution for Ad7 had a single peak between pH 6 and 7, indicating that Ad7 was in an endosomal compartment after endocytosis, similar to Ad5 (Fig. 3E). After a 30-min incubation, a new peak appeared at an acidic pH (Fig. 3F). The proportion of intracellular Ad7 at low pH increased in the first 2 h after infection and then decreased over the next 6 h (Fig. 3G to J). The decrease in the population of Ad7 at a low pH was matched by a corresponding increase in the population of Ad7 at neutral pH (Fig. 3I and J). The kinetics of Ad7 localization in compartments with different pHs indicated that Ad7 first entered a slightly acidic compartment, then moved to a more highly acidic compartment, and finally escaped to a neutral compartment.

Coincubation of Ad7 with α_2M. Ligands that enter cells via endocytosis are generally targeted either to the recycling pathway, leading to delivery back to the cell surface, or to the lysosomal pathway, leading to degradation (36). Well-characterized endocytic ligands that specifically enter either pathway include α_2M, which is targeted to the lysosomal pathway, and Tf, which is targeted to the recycling pathway. Sorting of these ligands into different pathways can be demonstrated by comparing their distribution at different times after internalization. Cy3-α_2M was partially colocalized with FITC-Tf in A549 cells after a 15-min coincubation with cells, reflecting cointernalization into sorting endosomes, an early, functionally distinct step in the endocytic pathway. When the cells were washed to remove unbound ligand after the 15-min incubation and were maintained at 37°C for an additional 45 min, the two endocytic ligands were located in distinct compartments (Fig. 4). This time course suggested that ligands destined for the lysosomal pathway left sorting endosomes and entered late endosomes within the first hour after internalization.

To determine whether Ad7 entered the lysosomal or the recycling pathway, the localization of Ad7 was compared with that of α_2M. Significant colocalization of carboxyfluorescein-Ad7 with Cy3-α_2M was observed 1 hr after infection (Fig. 5). Colocalization of Ad7 with α_2M could be detected up to 4 h after infection, indicating an extended residence time in an endocytic compartment in the lysosomal pathway.

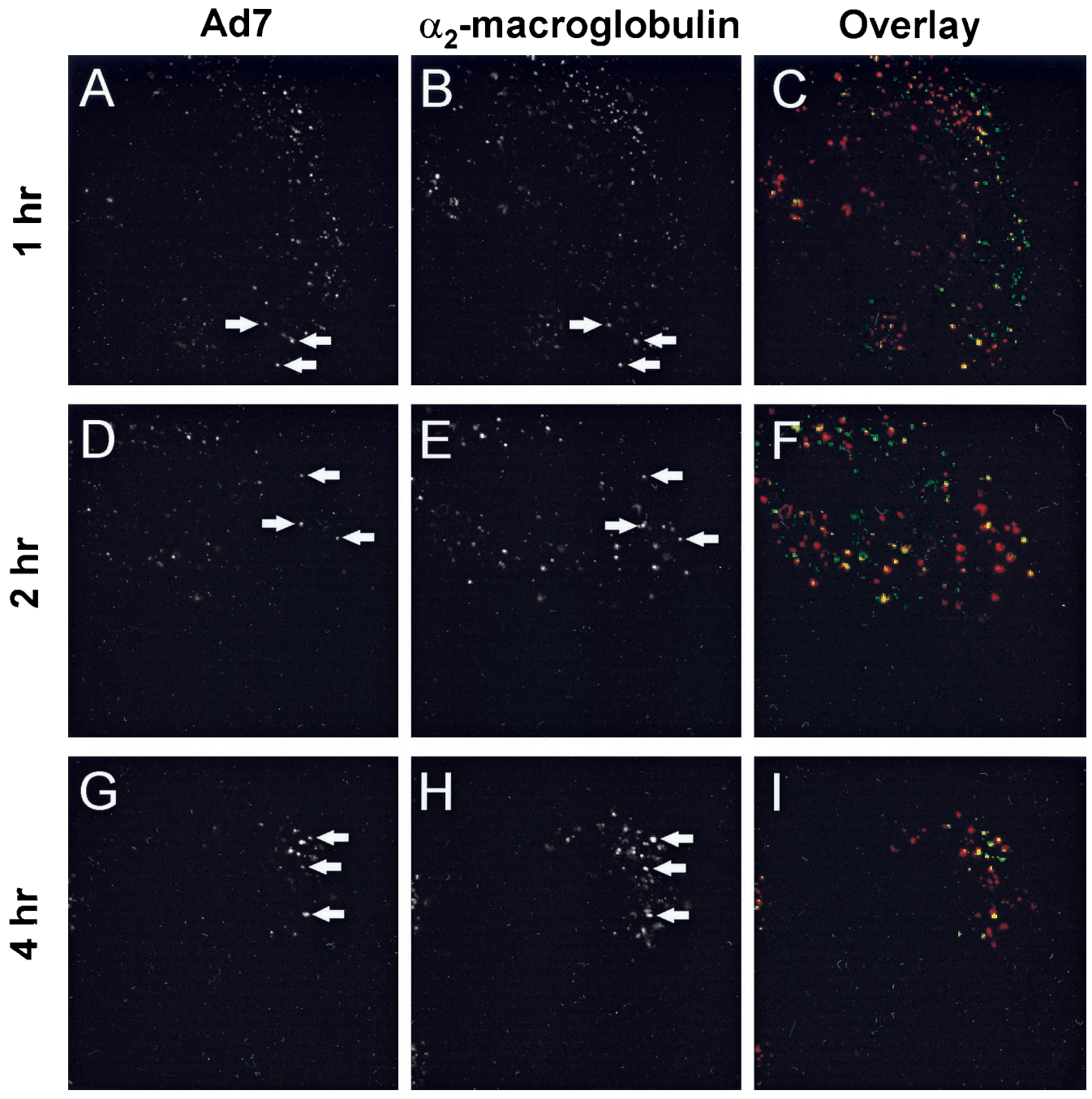

FIG. 5. Colocalization of Ad7 with α_2M. A549 cells were infected with carboxyfluorescein-Ad7 (10^{11} particles/ml) for 10 min at 37°C, loaded with Cy3-α_2M (10 μg/ml) for 15 min, and then incubated for an additional 45 or 105 min at 37°C. The left column shows carboxyfluorescein-Ad7, the center column shows Cy3-α_2M, and the right column shows a color overlap of the two signals (carboxyfluorescein-Ad7, green; Cy3-α_2M, red; colocalization yellow). (A) Carboxyfluorescein-Ad7, 1 h after infection. (B) Cy3-α_2M, 1 h after Ad7 infection, (C) Overlay of panels A and B. (D) Carboxyfluorescein-Ad7, 2 h after infection. (E) Cy3-α_2M, 2 h after Ad7 infection. (F) Overlay of panels D and E. (G) Carboxyfluorescein-Ad7, 4 h after infection (H) Cy3-α_2M, 4 h after Ad7 infection. (I) Overlay of panels G and H. Arrows indicate examples of colocalization of Ad7 and Cy3-α_2M. Field width, 50 μm.

Colocalization with endosomal and lysosomal proteins. Intracellular organelles can also be identified by their protein composition. Endosomes in the recycling pathway contain the Tf receptor, while endosomes in the lysosomal pathway are characterized by the presence of mannose-6-phosphate receptor and lysosome-associated membrane protein 1 (LAMP-1) (7, 20, 28). The endocytic compartments can also be distinguished by the Rab protein family of small GTP binding protein that are thought to regulate the trafficking of membrane and membrane-associated proteins among intracellular organelles (46). To identify the endosomal compartment in which Ad7 resides, A549 cells were infected with carboxyfluo-

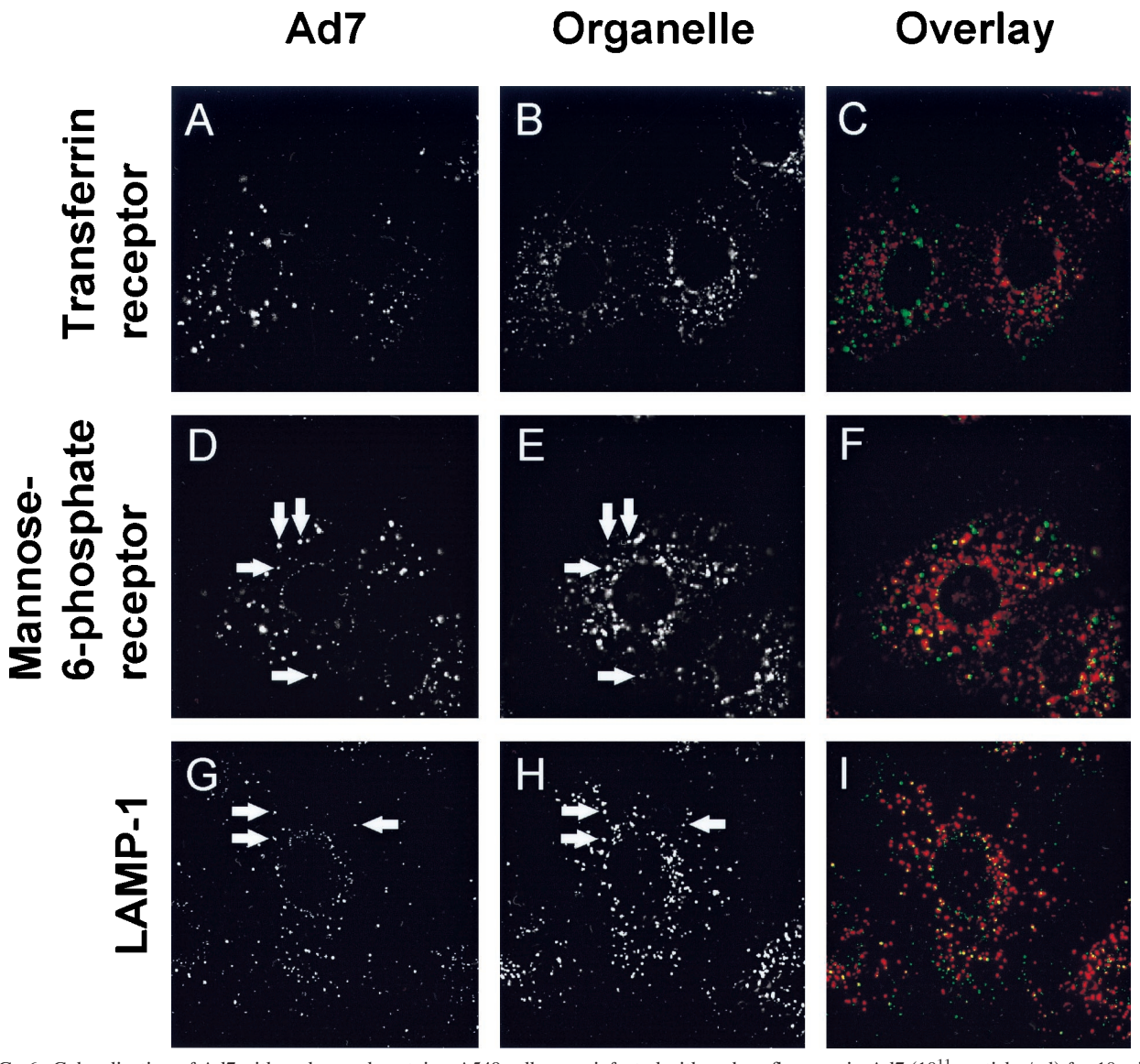

FIG. 6. Colocalization of Ad7 with endosomal proteins. A549 cells were infected with carboxyfluorescein-Ad7 (10^{11} particles/ml) for 10 min at 37°C, incubated for 60 min at 37°C, and then fixed and permeabilized. The cells were incubated at 23°C for 1 h with primary antibodies against Tf receptor, mannose-6-phospate receptor, or LAMP-1 and localized using Texas red-conjugated secondary antibodies. The left column shows carboxyfluorescein-Ad, the center column shows organelle-specific protein staining, and the right column shows overlap (Ad7, green; specific protein, red; overlap), yellow). Very little colocalization of Ad7 with Tf. receptor was observed. However, Ad7 was partially colocalized with mannose-6-phosphate (late endosomes) and LAMP-1 (late endosomes and lysosomes). Arrows indicate examples of colocalization. Field width, 40 μm.

rescein-Ad7 for 10 min and then incubated for 60 min; this was followed by indirect immunofluorescence localization of organelle markers. When Ad7 localization was compared with that of endosomal marker proteins, Ad7 was partially colocalized with markers of late endosomes and lysosomes (mannose-6-phosphate receptor and LAMP-1), but not with the recycling endosome marker, Tf receptor (Fig. 6). Consistent with this finding, Ad7 was partially colocalized with Rab 7, a marker of late endosomes, but not with Rab 4, 5, or 11, which are associated with recycling, sorting, and apical recycling endosomes, respectively (Fig. 7).

Rapid, linear translocations of Ad5 and Ad7. It is known that Ad5 is capable of rapid, linear translocations in cytosol following escape from endosomes (26, 27, 49). To determine whether Ad7 also exhibited rapid intracellular motility, a series of images of infected cells were acquired at two time points after infection, 30 min and 4 h (Fig. 8). Ad5 motility at 30 min (0.29 ± 0.07 translocations/virus/min) was comparable to previously reported values at this time point (27). Ad5 motility observed 4 h after infection was significantly decreased compared to that at the 30-min time point ($P < 0.01$), probably reflecting the high degree of stable association of Ad5 capsids

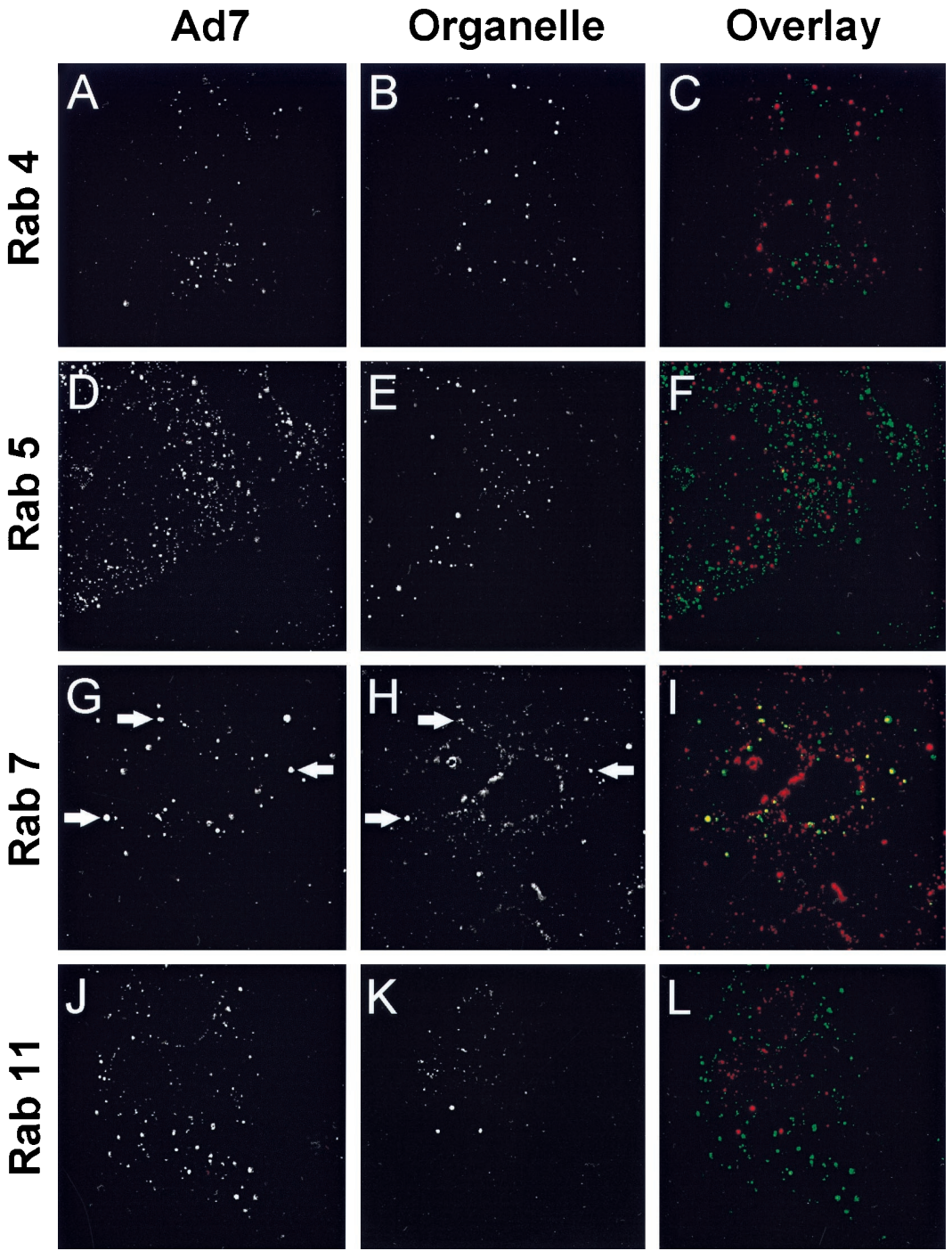

FIG. 7. Colocalization of Ad7 with small GTP binding proteins found in late endosomes and lysosomes. A549 cells were infected with carboxyfluorescein-Ad7 (10^{11} particles/ml) for 10 min at 37°C, incubated for 60 min at 37°C, and then fixed and permeabilized. The cells were incubated at 23°C for 1 h with primary antibodies against Rab proteins, using Texas red-conjugated secondary antibodies. The left column shows carboxyfluorescein-Ad, the center column shows organelle-specific protein staining, and the right column shows overlap (Ad7, green; specific protein, red; colocalization, yellow). Very little colocalization of Ad7 with Rab 4, Rab 5, or Rab 11 was observed. However, Ad7 was partially colocalized with Rab 7 (late endosomes and lysosomes). Arrows indicate examples of colocalization. Field width, 40 μm.

with the nuclear envelope late in the infection. In contrast, the motility of Ad7 was lower than that of Ad5 30 min after infection but increased rather than decreased by the 4-h time point, such that Ad7 motility 4 h after infection was significantly higher than either Ad5 motility at that time point or Ad7 motility at the earlier time point ($P < 0.01$ and $P < 0.05$, respectively), probably reflecting an increase in the Ad7 population free in cytosol.

Influence of Ad7 fiber protein on the pH optimum for membrane lysis by Ad. Intracellular trafficking of Ad7 appears

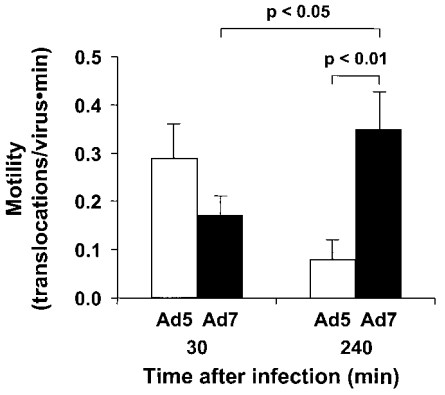

FIG. 8. Quantitative comparison of the motility of Ad5 and Ad7 at different time points. A549 cells were infected with Cy3-Ad5 or Cy3-Ad7 (10^{11} particles/ml) for 10 min, at 37°C, washed out, and incubated at 37°C for 30 or 240 min. Digital segments of the fluorescent image fields were analyzed with respect to the number of linear translocations (>2 μm) observed. Data are normalized with respect to the number of viruses visible in the field and the duration of observation. The motility of Ad7 at 240 min after infection was increased significantly compared with that 30 min after infection, whereas the motility of Ad5 decreased over the same interval.

distinct from trafficking of Ad5 in that Ad7 entered a low-pH compartment while Ad5 rapidly escaped to the pH-neutral cytosol. These observations led to the hypothesis that Ad7 would exhibit a shift toward a lower pH for optimum membrane lysis compared to Ad5. To aid in this analysis, we used a chimeric Ad capsid composed of a complete Ad5 capsid with an Ad7 fiber protein substituted for the Ad5 fiber protein (Ad5fiber7) [16]; the Ad57 fiber vector was previously noted to have intracellular trafficking characteristics similar to those of Ad7 rather than Ad5 (33). The availability of this chimera allowed a test of the hypothesis that the Ad7 fiber protein would confer this property onto the Ad5fiber7 chimeric capsid. Previous reports showed that Ad5 was capable of lysing cell membranes with a pH optimum of 6.0, using an experimental model in which Ad capsids were bound to the plasma membrane of KB cells that had been loaded with [^{3}H]choline (4, 43, 44). Capsid binding was performed in the presence of sodium azide to eliminate cytosolic ATP and prevent endocytosis. Release of ^{3}H to the supernatant was taken as a measure of cell lysis. KB cells were used for this assay rather than A549 cells because A549 cells exhibited an unacceptably high rate of spontaneous cell lysis at pH values below 6.0 (data not shown).

[^{3}H]choline release was strongly dependent on the pH of the medium for both Ad5, Ad7, and the chimeric Ad5fiber7 (Fig. 9). The activity of Ad5-induced cell membrane lysis was most effective at pH 6.0, in agreement with previously published reports (4, 43, 44). At this pH, lysis induced by Ad5 was significantly greater than lysis induced by Ad7 or Ad5fiber7 ($P < 0.05$). Interestingly, the lytic activity of Ad7 was most effective at pH 5.5, even though the Ad5 lytic activity was lost at that pH value. The Ad7-induced lysis was significantly greater than Ad5 at pH 5.5 ($P > 0.05$), indicating that the endosome disruption by Ad7 was optimal in low-pH compartments. The Ad5fiber7 chimera also exhibited a pH optimum of 5.5 for membrane lysis, with significantly more lysis than Ad5 ($P < 0.05$), suggesting that the fiber protein confers the characteristics of membrane lysis on the capsid.

DISCUSSION

While Ad5 and Ad7 both use receptor-mediated endocytosis to enter cells, the routes by which they deliver their genomes to the nucleus are quite distinct. The hallmark of a subgroup C Ad infection is rapid escape to the cytosol following internalization by receptor-mediated endocytosis (6, 15). This has been characterized for subgroup C serotypes 1, 2 and 5, but this property is clearly not shared universally among members of the *Adenoviridae* family. In particular, members of subgroup B (serotypes 3 and 7) are noted for their relatively long residence times inside membranous organelles, identified as lysosomes based on the ultrastructural appearance of the organelle or cosedimentation of the viral genome with lysosomal markers (6, 37). The present study has focused on a functional characterization of the compartments through which Ad7 traffics using colocalization of virions with compartment markers, compartment pH, and membrane lysis. The data clearly identify the lysosomal pathway as the route used by Ad7 virions. Despite trafficking through this pathway, Ad7 has the ability to escape degradation in these organelles. Interestingly, the data show that Ad7 traffics through the low pH lysosomal pathway and that the fiber protein confers the property of low-pH escape of the Ad7 capsid to the cytoplasm (Fig. 10).

Delivery of Ad7 to functionally characterized endosomes in the lysosomal pathway. The functional characterization of Ad7 infection included the observations that Ad7-containing compartments had a low luminal pH and contained endocytic ligands known to traffic to lysosomes. One functional definition of late endosomes and lysosomes is acidification of the organelle interior below pH 6.0. Ad5 virions remained at or slightly below neutrality throughout infection, including time

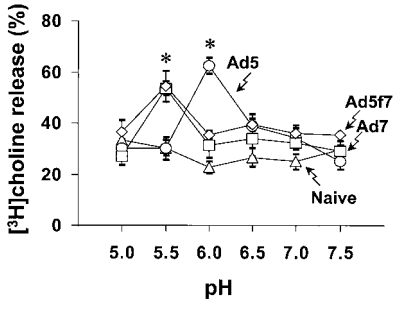

FIG. 9. Effect of pH on Ad-dependent membrane lysis. KB cells (2×10^4 cells) were incubated for 1 h in medium containing [^{3}H]choline, washed, chilled to 4°C, and then treated with 10^{11} particles of Ad5, Ad7, or the chimeric virus Ad5fiber7 for 1 h. The medium was replaced with permeability buffer at various pH, containing sodium azide to prevent endocytosis of the viruses. Cells with bound viruses were then warmed to 37°C for 1 h to permit lysis. The percent [^{3}H]choline release was determined by measuring ^{3}H released into the medium compared with the counts remaining in cells. Data from Ad5, Ad7, Ad5fiber7 (Ad5f7), and naive control are shown as mean values ± standard error. The activity of Ad5-induced membrane lysis was significantly greater than that of Ad7- or Ad5fiber7-induced lysis at pH 6.0; the activity of Ad5-induced membrane lysis was significantly less than that of Ad7- or Ad5fiber7-induced lysis at pH 5.5 ($P < 0.05$ for each comparison).

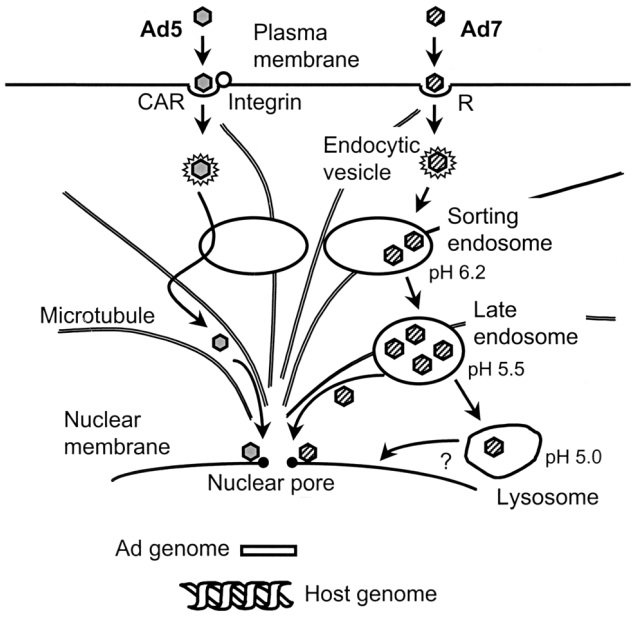

FIG. 10. Summary of intracellular trafficking of subgroup B and subgroup C Ad. Subgroup C Ad (e.g., Ad5) is internalized via interaction with a high affinity receptor (coxsackie-virus-Ad receptor [CAR]) and a secondary receptor integrin and then enters the cell via receptor-mediated endocytosis. When the endocytic compartment containing Ad5 fuses with a sorting endosome (pH 6.2), Ad5 breaks out the early endosome, escapes to the cytosol, and translocates to the nucleus along microtubules within 1 h. Subgroup B Ad (e.g., Ad7) binds to cells via interaction with an unidentified receptor (R) and is internalized via receptor-mediated endocytosis. The endocytic compartment containing Ad7 fuses with sorting endosomes, but unlike Ad5, Ad7 does not disrupt the sorting-endosome membrane, remaining inside that organelle as it matures to become a late endosome (pH 5.5) and finally a lysosome (pH 5.0). Ad7 escapes from late endosomes and/or lysosomes and translocates to the nucleus. Following equally rapid internalization ($t_{1/2}$ = 2 to 3 min) (33), Ad5 reaches the nucleus rapidly ($t_{1/2}$ = 40 min) while Ad7 trafficking progresses more slowly ($t_{1/2}$ = 220 min).

points 10 min after infection (when previous studies have shown that all of the Ad5 virions had been internalized) and 60 min after infection (when previous studies have shown that 70 to 80% of Ad5 virions were associated with the nuclear envelope) (26, 33). In contrast, Ad7 rapidly entered acidic compartments, with approximately 30% of virions residing in compartments of pH $<$ 6.0 within 30 min after infection. That percentage grew to a maximum of approximately 50% 2 h after infection. Since pH $<$ 6.0 is indicative of late endosomes and lysosomes, these data suggest that Ad7 entered compartments that exhibited a functional property of the lysosomal pathway.

A second functional characteristic of the lysosomal pathway that was examined in A549 cells was sorting of endocytic ligands. Fluorescence microscopy of Cy3-Ad5 virions showed that the Ad5 retained a uniform size throughout the cell, while imaging of Ad7 revealed an increase in the size of the fluorescent puncta. The data showed that these sites of local accumulation of Ad7 corresponded to α_2M-containing compartments. The fact that the α_2M-containing compartment diverged from cointernalized Tf 45 min after addition of labeled α_2M provided a functional demonstration that the α_2M-containing compartments mature to become late endosomes destined for fusion with primary lysosomes. Colocalization of Ad7 with α_2M at time points from 60 to 240 min after infection agreed with the time course of Ad7 localization in low-pH compartments.

Colocalization of Ad7 with late endosome- and lysosome-associated proteins. Subcellular localization of virions can be accomplished using reagents such as antibodies that mark the position of organelle-specific proteins. Using this strategy, Ad7 localization was compared with the subcellular distribution of three proteins which mark different parts of the endocytic system: Tf receptor, a transmembrane protein that binds Tf and carries it through the endocytic recycling compartment (9); mannose-6-phosphate receptor, a protein that is located primarily in late endosomes (24); and LAMP-1, a protein found in late endosomes and lysosomes (7, 28). At 1 h after infection, Ad7 showed partial colocalization with mannose-6-phosphate receptor and LAMP-1, confirming delivery of Ad7 to late endosomes and lysosomes.

A family of small GTP-binding proteins, the Rab proteins, participate in membrane trafficking among distinct intracellular compartments, and organelle-specific localization of several members of the Rab family has been demonstrated (46). Using antibodies to Rab 5 (which marks an early endosome in which sorting of ligands and receptors occurs), Rab 4 (the recycling endosomes that holds material destined for return to the cell surface), Rab 11 (specialized recycling endosomes found in epithelial cells), and Rab 7 (late endosomes), Ad7 was found to colocalize only with Rab 7, supporting the observation that Ad7 trafficked to late endosomes.

The examples of colocalization between Ad7 and compartment markers uniformly resulted in partial rather than complete colocalization of the two fluorescent signals. This result was probably a consequence of the biology of Ad7. First, Ad7, being an infectious agent, has the property of lysing an endosomal compartment and escaping to the cytosol (8). Thus, some fraction of the Ad7 signal will always fail to colocalize with organelle markers since the organelle markers will not correspond to Ad7 which has escaped. Second, Ad7 was applied to cells for only 10 min, leading to a wave of viral infection. As such, the Ad7 would be expected to correspond only to a subset of late endosomes or lysosomes that were formed as the wave of Ad7 reached that stage of the endocytic pathway. As a result, the examples of partial colocalization illustrated in this report logically reflect localization of an infectious agent during a dynamic process.

Functional significance and mechanism of Ad7 trafficking to late endosomes and lysosomes. Subgroup B Ad are noted for their comparatively low efficiency is establishing an infection (11). Subgroup B viruses often have particle-to-PFU ratios 10-fold higher than those of subgroup C viruses (1, 11). One interpretation of the high particle-to-PFU ratio is that fewer incoming viruses are infective, a model that would be favored if degradation of lysosome-targeted virions were observed. The present data do not support this interpretation. Instead, the data suggest that no loss of viral genome occurs during virion residence in low-pH compartments (0 to 8 h after infection), that the viral genome is quantitatively delivered to the nucleus, and that delivery to a low-pH compartment favors escape to the cytosol. These data, in combination with previous data

showing that gene transfer vectors based on the Ad7 capsid are equally efficient in terms of gene transfer compared with Ad5-based gene transfer vectors (1), argue strongly that the infection pathway of Ad in subgroup B, while different from that of Ad in subgroup C, is equally competent for delivery of the genome to the nucleus. In this context, the difference in infection efficiency of the subgroups indicated by titer assays probably reflects some other aspect of the viral life cycle, such as capsid assembly.

The mechanism governing effective Ad intracellular trafficking is highly dependent on the ability of the Ad capsid to escape from endosomes. For virions from subgroup C, which exhibit rapid escape from endosomes, the probability of endosome escape is likely to increase in acidic compartments. This concept is based on previous demonstrations that Ad-mediated endosomal lysis is enhanced at a pH of 6.0 (corresponding to the pH observed in early endosomes) and observations that inhibition of endosome acidification prevents infection (17, 26, 38). Based on the observation that anti-penton antibody suppresses the ability of subgroup C to lyse membranes in vitro, penton base protein has been linked to the lytic activity of these Ad (44, 56). The data generated in the present study suggest that the fiber protein may also play an important intracellular role during infection, perhaps acting as a pH sensor which triggers the endosomal lytic activity. This interpretation stems from observations showing Ad5 and Ad7 escape from early and late endosomal compartments, respectively. This property appears to be based on the fact that the viral DNA is transferred quantitatively to the nucleus with distinct kinetics for escape from early or late endosomes. Remarkably, the properties of localized intracellular accumulation, colocalization with an endocytic ligand destined for lysosomes (α_2M), and slowed kinetics of DNA delivery to the nucleus are all conferred on a chimeric capsid composed entirely of Ad5 proteins with the exception of the fiber protein which comes from Ad7 (16). The data also show that the fiber has the additional property of defining the pH optimum for membrane lysis. Taken together, the simplest interpretation of the data is that the properties of the fiber protein control the timing of endosomal escape and, in doing so, govern the extent to which the capsid traffics within endocytic compartments prior to escape to the cytosol. A role for fiber after binding is supported by the observations of Legrand et al. (25), who compared the infection efficiency of normal fiber-bearing Ad capsids to that of fiberless Ad capsids in cells that lacked a high-affinity receptor for the fiber protein and found that fiber-containing Ad was 100-fold more infective than was fiberless Ad.

An alternative interpretation of the data is that the fiber protein is directly responsible for lysis of the endosome. While it is clear that the penton base interaction with integrin facilitates entry and that inhibition of that interaction can prevent membrane lysis (43, 56), the enzymatic activity required for lysis of endosomal membranes has never been unambiguously assigned to any one capsid protein. The fact that the recombinant penton base protein competitively inhibits Ad-mediated lysis of cells rather than causing lysis itself also argues that the penton base, while necessary for lysis, may not be sufficient (56). It is similarly unlikely that the fiber protein alone can induce lysis of membranes, given the observations that the affinity of fiber for membranes decreases in the pH range found in early endosomes (50), that high concentrations of purified or recombinant fiber protein have been exposed to cells without mention of toxicity (48, 57), and that fiberless capsids are still able to accomplish infection, albeit at significantly reduced efficiency (25, 53). If the penton base and fiber are both necessary for lysis yet neither is sufficient to accomplish lysis independently, the penton base-fiber complex may be required. Support for this model comes from the work of Fender et al. (14), who showed that penton base-fiber dodecahedrons efficiently bound to cells and translocated to the nucleus, suggesting that membrane lysis was accomplished.

The difference in the half time of delivery of Ad7 and Ad5 to the nucleus was observed at both high and low multiplicities of infection, indicating that Ad7 trafficking through late endosomes was not an artifact of high viral concentrations during infection. Morphological observations of Ad7 trafficking (Ad7 colocalization with compartment markers; determination of the pH of Ad7-containing compartments) were performed following a brief (10-min) infection of cells at a very high multiplicity of infection (30,000 particles per cell). These results showed a long-lived association of Ad7, but not Ad5, with late endosomal compartment markers and low-pH compartments. Similar observations with nonfluorescent Ad7 were reported previously using in situ hybridization to localize Ad genome in cells up to 8 h after infection (33). Time-resolved data from both the pH determinations and in situ hybridization showed that the majority of Ad7 did not escape from cytoplasmic compartments for several hours after infection. Brief (10-min) infections with a low multiplicity of infection (1,000 particles per cell) were used in a quantitative determination of the rate of Ad genome transfer to the nucleus. Despite the 30-fold difference in the concentration of virus during infection, a similar rate of translocation of the Ad genome to the nucleus was observed (2 to 3 h half time). Interestingly, the Ad7 genome was observed to begin encountering the nucleus as early as 1 h postinfection by the quantitative PCR assay, a finding in agreement with the observation of a minority of vector in association with the nuclear envelope at this time point.

Late stages in infection. After escape from endosomes, Ad translocates to the nucleus and binds to the nuclear envelope. Subgroup C capsids translocate at rates up to 2 μm/s in living cells, using the microtubule-dependent motor protein, cytoplasmic dynein, to mediate Ad motility in cytosol following Ad escape from endosomes (26, 27, 49). Like subgroup C Ad, Ad7 exhibited rapid intracellular movements, but the number of Ad7 movements increased over the course of a 4-h incubation while the number of Ad5 movements decreased, possibly reflecting the slower kinetics of Ad7 release to the cytosol. The rapid movement of Ad7 suggests that Ad7 may also interact with microtubule-based motor molecules. Combined with a previous observation that Ad5 and Ad7 share a similar binding mechanism with the nuclear envelope (58), it is likely that the mechanism of infection of subgroups B and C are quite similar following escape to the cytosol.

Targeting gene therapy vectors to cells. Utilization of gene transfer vectors in vivo has been limited to some extent by the native tropism of viral vectors. In Ad, early dependence on subgroup C-based vectors limited the vector tropism to cells with accessible receptors for subgroup C vectors. To expand the host range of subgroup C vectors, capsids have been retar-

geted by incorporating novel affinities for cell surface molecules into the capsid structure (55). Given that subgroup B Ad have a different cell surface receptor from subgroup C Ad (11, 16, 33, 39, 48), a series of chimeric vectors have been produced to take advantage of the difference in viral receptors between subgroups. Chimeric Ad vectors expressing either an Ad3 knob/Ad5 shaft fiber protein or full-length Ad3 fiber protein exhibit increased transduction of human fibroblasts, monocytes, B-lymphoid cell lines, or squamous carcinoma cell lines compared to subgroup C Ad vectors (47, 54). The chimeric Ad5fiber7 vector used in this study demonstrates subgroup B-specific binding (16, 33) as well as altered in vivo tropism (16). While the potential advantages of altering tropism are evident, the possible contributions of altered intracellular trafficking of subgroup B/C chimeric capsids remain to be evaluated.

Targeting gene therapy vectors to lysosomes? Although the concept of purposely targeting a gene transfer vector to a lysosome may be counterintuitive, the fact remains that many advances in the development of nonviral gene transfer vectors (vectors composed of plasmid DNA complexed with lipids, polymers, and or peptides) have relied on mimicking the infection pathway of viruses. One significant problem plaguing the development of nonviral vectors has been intracellular translocation of plasmids to the nuclei of cells, since plasmids exhibit poor diffusion characteristics in the cytoplasm (12, 29). Evolution has conferred upon viruses highly efficient technological strategies for delivering genomes to nuclei of eukaryotic cells. For example, by utilizing a pH-triggered lysis mechanism, virions are less apt to undergo irreversible capsid changes required for infection while the capsid remains outside of the target cell. Targeting to the lysosomal pathway and delayed escape from endosomes may permit Ad7 to take advantage of host cell mechanisms for moving material through the cytoplasm to the nucleus. Ad capsids, like plasmids, are not capable of rapid diffusion in the cytoplasm (27), so the capsid must find mechanisms for translocating to the nucleus. Ad2 and Ad5 utilize microtubule-based molecular motors to achieve nuclear localization after escape to the cytosol (27, 49). Ad7, conversely, may accomplish nuclear localization, in part, by remaining inside late endosomes and lysosomes, since these organelles are often transported toward nuclei (e.g., prelysosomal organelles in the axons of neurons are transported specifically toward the cell body). Ad7 may achieve greater proximity to the nucleus by remaining inside late endosomes and lysosomes prior to escape to the cytosol. Nonviral vector designers have devised mechanisms for conveying receptor-specific mechanisms for binding nonviral vectors to the cell surface, have incorporated pH-enhanced fusion mechanisms, and have conjugated nuclear localization sequences to synthetic vectors. Thus, it stands to reason that if a nonviral vector containing a plasmid could be engineered to remain in the lysosomal pathway for an extended period prior to escape, the plasmid may be released near the nucleus, thereby increasing the transduction efficiency of the vector.

ACKNOWLEDGMENTS

We thank W. Van't Hof, F. R. Maxfield, W. Mallet (all from Weill Medical College of Cornell University), L. Traub (Washington University), T. Wickham (GenVec), and S. Simon (Rockefeller University) for valuable discussions, and we thank N. Mohamed for help in preparing the manuscript.

These studies were supported, in part, by NIH grants P01 HL51746-06A1 and P01 HL59312; the Will Rogers Memorial Fund, Los Angeles, Calif.; the Cystic Fibrosis Foundation, Bethesda, Md.; and GenVec, Inc., Rockville, Md. P.L.L. is also supported in part by NIH grant R29AI 42250.

REFERENCES

1. **Abrahamsen, K., H. L. Kong, A. Mastrangeli, D. Brough, A. Lizonova, R. G. Crystal, and E. Falck-Pedersen.** 1997. Construction of an adenovirus type 7a Ela vector. J. Virol. **71:**8946–8951.
2. **Bai, M., B. Harfe, and P. Freimuth.** 1993. Mutations that alter an Arg-Gly-Asp (RGD) sequence in the adenovirus type 2 penton base protein abolish its cell-rounding activity and delay virus reproduction in flat cells. J. Virol. **67:**5198–5205.
3. **Bergelson, J. M., J. A. Cunningham, G. Droguett, E. A. Kurt-Jones, A. Krithivas, J. S. Hong, M. S. Horwitz, R. L. Crowell, and R. W. Finberg.** 1997. Isolation of a common receptor for coxsackie B viruses and adenoviruses 2 and 5. Science **275:**1320–1323.
4. **Blumenthal, R., P. Seth, M. C. Willingham, and I. Pastan.** 1986. pH-dependent lysis of liposomes by adenovirus. Biochemistry **25:**2231–2237.
5. **Chardonnet, Y. and S. Dales.** 1970a. Early events in the interaction of adenoviruses with HeLa cells. I. Penetration of type 5 and intracellular release of the DNA genome. Virology **40:**462–477.
6. **Chardonnet, Y. and S. Dales.** 1970b. Early events in the interaction of adenoviruses with HeLa cells. II. Comparative observations on the penetration of types 1, 5, 7, and 12. Virology **40:**478–485.
7. **Chen, J. W., T. L. Murphy, M. C. Willingham, I. Pastan, and J. T. August.** 1985. Identification of two lysosomal membrane glycoproteins. J. Cell Biol. **101:**85–95.
8. **Dales, S.** 1962. An electron microscope study of the early association between two mammalian viruses and their roles. J. Cell Biol. **13:**303–322.
9. **Dautry-Varsat, A., A. Ciechanover, and H. F. Lodish.** 1983. pH and the recycling of transferrin during receptor-mediated endocytosis. Proc. Natl. Acad. Sci. USA **80:**2258–2262.
10. **Davison, E., R. M. Diaz, I. R. Hart, G. Santis, and J. F. Marshall.** 1997. Integrin $\alpha_5\beta_1$-mediated adenovirus infection is enhanced by the integrin-activating antibody TS2/16. J. Virol. **71:**6204–6207.
11. **Defer, C., M. T. Belin, M. L. Caillet-Boudin, and P. Boulanger.** 1990. Human adenovirus-host cell interactions: comparative study with members of subgroups B and C. J. Virol. **64:**3661–3673.
12. **Dowty, M. E., P. Williams, G. Zhang, J. E. Hagstrom, and J. A. Wolff.** 1995. Plasmid DNA entry into postmitotic nuclei of primary rat myotubes. Proc. Natl. Acad. Sci. USA **92:**4572–4576.
13. **Dunn, K. W., S. Mayor, J. N. Myers, and F. R. Maxfield.** 1994. Applications of ratio fluorescence microscopy in the study of cell physiology. FASEB J. **8:**573–582.
14. **Fender, P., R. W. Ruigrok, E. Gout, S. Buffet, and J. Chroboczek.** 1997. Adenovirus dodecahedron, a new vector for human gene transfer. Nat. Biotechnol. **15:**52–56.
15. **FitzGerald, D. J., R. Padmanabhan, I. Pastan, and M. C. Willingham.** 1983. Adenovirus induced release of epidermal growth factor and pseudomonas toxin into the cytosol of KB cells during receptor-mediated endocytosis. Cell **32:**607–617.
16. **Gall, J., A. Kass-Eisler, L. Leinwand, and E. Falck-Pedersen.** 1996. Adenovirus type 5 and 7 capsid chimera: fiber replacement alters receptor tropism without affecting primary immune neutralization epitopes. J. Virol. **70:**2116–2123.
17. **Greber, U. F., M. Willetts, P. Webster, and A. Helenius.** 1993. Stepwise dismantling of adenovirus 2 during entry into cells. Cell **75:**477–486.
18. **Greber, U. F., P. Webster, J. Weber, and A. Helenius.** 1996. The role of the adenovirus protease on virus entry into cells. EMBO J. **15:**1766–1777.
19. **Greber, U. F., M. Suomalainen, R. P. Stidwill, K. Boucke, M. W. Ebersold, and A. Helenius.** 1997. The role of the nuclear pore complex in adenovirus DNA entry. EMBO J. **16:**5998–6007.
20. **Griffiths, G., B. Hoflack, K. Simons, I. Mellman, and S. Kornfeld.** 1988. The mannose 6 phosphate receptor and the biogenesis of lysosomes. Cell **52:**329–341.
21. **Horwitz, M. S.** 1996. Adenoviruses, p. 2149–2171. *In* B. N. Fields, D. M. Knipe, and P. M. Howley (ed.), Fields virology. Lippincott-Raven Publishers, Inc., Philadelphia, Pa.
22. **Huang, S., T. Kamata, Y. Takada, Z. M. Ruggeri, and G. R. Nemerow.** 1996. Adenovirus interaction with distinct integrins mediates separate events in cell entry and gene delivery to hematopoietic cells. J. Virol. **70:**4502–4508.
23. **Kass-Eisler, A., E. Falck-Pedersen, M. Alvira, J. Rivera, P. M. Buttrick, B. A. Wittenberg, L. Cipriani, and L. A. Leinwand.** 1993. Quantitative determination of adenovirus-mediated gene delivery to rat cardiac myocytes in vitro and in vivo. Proc. Natl. Acad. Sci. USA **90:**11498–11502.
24. **Klausner, R. D., G. Ashwell, J. van Renswoude, J. B. Harford, and K. R. Bridges.** 1983. Binding of apotransferrin to K562 cells: explanation of the

transferrin cycle. Proc. Natl Acad. Sci. USA **80:**2263–2266.
25. **Legrand, V., D. Spehner, Y. Schlesinger, N. Settelen, A. Pavirani, and M. Mehtali.** 1999. Fiberless recombinant adenoviruses: virus maturation and infectivity in the absence of fiber. J. Virol. **73:**907–919.
26. **Leopold, P. L., B. Ferris, I. Grinberg, S. Worgall, N. R. Hackett, and R. G. Crystal.** 1998. Fluorescent virions: dynamic tracking of the pathway of adenoviral gene transfer vectors in living cells. Hum. Gene Ther. **9:**367–378.
27. **Leopold, P. L., G. Kreitzer, N. Miyazawa, S. Rempel, K. K. Pfister, E. Rodriguez-Boulan, and R. G. Crystal.** 2000. Dynein- and microtubule-mediated translocation of adenovirus serotype 5 occurs after endosomal lysis. Hum. Gene Ther. **11:**151–165.
28. **Lippincott-Schwartz, J. and D. M. Fambrough.** 1987. Cycling of the integral membrane glycoprotein, LEP100, between plasma membrane and lysosomes: kinetic and morphological analysis. Cell **49:**669–677.
29. **Lukacs, G. L., P. Haggie, O. Seksek, D. Lechardeur, N. Freedman, and A. S. Verkman.** 2000. Size-dependent DNA mobility in cytoplasm and nucleus. J. Biol Chem. **275:**1625–1629.
30. **Mathias, P., M. Galleno, and G. R. Nemerow.** 1998. Interactions of soluble recombinant integrin alphav beta5 with human adenoviruses. J. Virol. **72:** 8669–8675.
31. **Maxfield, F. R.** 1982. Weak bases and ionophores rapidly and reversibly raise the pH of endocytic vesicles in cultured mouse fibroblasts. J. Cell Biol. **95:**676–681.
32. **Maxfield, F. R.** 1989. Measurement of vacuolar pH and cytoplasmic calcium in living cells using fluorescence microscopy. Methods Enzymol. **173:**745–771.
33. **Miyazawa, N., P. L. Leopold, N. R. Hackett, B. Ferris, S. Worgall, E. Falck-Pedersen, and R. G. Crystal.** 1999. Fiber swap between adenovirus subgroups B and C alters intracellular trafficking of adenovirus gene transfer vectors. J. Virol. **73:**6056–6065.
34. **Morgan, C., H. S. Rosenkranz, and B. Mednis.** 1969. Structure and development of viruses as observed in the electron microscope. V. Entry and uncoating of adenovirus. J. Virol. **4:**777–796.
35. **Muggeridge, M. I., and N. W. Fraser.** 1986. Chromosomal organization of the herpes simplex virus genome during acute infection of the mouse central nervous system. J. Virol. **59:**764–767.
36. **Mukherjee, S., R. N. Ghosh, and F. R. Maxfield.** 1997. Endocytosis. Physiol. Rev. **77:**759–803.
37. **Ogier, G., Y. Chardonnet, and W. Doerfler.** 1977. The fate of type 7 adenovirions in lysosomes of HeLa cells. Virology **77:**66–77.
38. **Prchla, E., C. Plank, E. Wagner, D. Blaas, and R. Fuchs.** 1995. Virus-mediated release of endosomal content in vitro: Different behavior of adenovirus and rhinovirus serotype 2. J. Cell Biol. **131:**111–123.
39. **Roelvink, P. W., A. Lizonova, J. G. Lee, Y. Li, J. M. Bergelson, R. W. Finberg, D. E. Brough, I. Kovesdi, and T. J. Wickham.** 1998. The coxsackievirus-adenovirus receptor protein can function as a cellular attachment protein for adenovirus serotypes from subgroups A, C, D, E, and F. J. Virol. **72:**7909–7915.
40. **Rosenfeld, M. A., W. Siegfried, K. Yoshimura, K. Yoneyama, M. Fukayama, L. E. Stier, P. K. Paakko, P. Gilardi, L. D. Stratford-Perricaudet, M. Perricaudet, S. Jallat, A. Pavirani, J.-P. Lecocq, and R. G. Crystal.** 1991. Adenovirus-mediated transfer of a recombinant α1-antitrypsin gene to the lung epithelium in vivo. Science **252:**431–434.
41. **Rosenfeld, M. A., K. Yoshimura, B. C. Trapnell, K. Yoneyama, E. R. Rosenthal, W. Dalemans, M. Fukayama, J. Bargon, L. E. Stier, L. Stratford-Perricaudet, M. Perricaudet, W. B. Guggino, A. Pavirani, J.-P. Lecocq, and R. G. Crystal.** 1992. In vivo transfer of the human cystic fibrosis transmembrane conductance regulator gene to the airway epithelium. Cell **68:**143–155.
42. **Saphire, A. C., T. Guan, E. C. Schirmer, G. R. Nemerow, and L. Gerace.** 2000. Nuclear import of adenovirus DNA in vitro involves the nuclear protein import pathway and hsc 70. J. Biol. Chem. **275:**4298–4304.
43. **Seth, P.** 1994. Adenovirus-dependent release of choline from plasma membrane vesicles at an acidic pH is mediated by the penton base protein. J. Virol. **68:**1204–1206.
44. **Seth, P., M. C. Willingham, and I. Pastan.** 1984. Adenovirus-dependent release of ^{51}CR from KB cells at an acidic pH. J. Biol. Chem. **259:**14350–14353.
45. **Shenk, T.** 1996. Adenoviridae: The viruses and their replication, p. 2111–2148. *In* B. N. Fields, D. M. Knipe, and P. M. Howley (ed.), Field Virology. Lippincott-Raven Publishers, Inc., Philadelphia, Pa.
46. **Somsel, R. J., and A. Wandinger-Ness.** 2000. Rab GTPases coordinate endocytosis. J. Cell Sci. **113:**183–192.
47. **Stevenson, S. C., M. Rollence, J. Marshall-Neff, and A. McClelland.** 1997. Selective targeting of human cells by a chimeric adenovirus vector containing a modified fiber protein. J. Virol. **71:**4782–4790.
48. **Stevenson, S. C., M. Rollence, B. White, L. Weaver, and A. McClelland.** 1995. Human adenovirus serotypes 3 and 5 bind to two different cellular receptors via the fiber head domain. J. Virol. **69:**2850–2857.
49. **Suomalainen, M., M. Y. Nakano, S. Keller, K. Boucke, R. P. Stidwill, and U. F. Greber.** 1999. Microtubule-dependent plus- and minus end-directed motilities are competing processes for nuclear targeting of adenovirus. J. Cell Biol. **144:**657–672.
50. **Svensson, U.** 1985. Role of vesicles during adenovirus 2 internalization into HeLa cells. J. Virol. **55:**442–449.
51. **Thomas, J. A., R. N. Buchsbaum, A. Zimniak, and E. Racker.** 1979. Intracellular pH measurements in Ehrlich ascites tumor cells utilizing spectroscopic probes generated in situ. Biochemistry **18:**2210–2218.
52. **Tomko, R. P., R. Xu, and L. Philipson.** 1997. HCAR and MCAR: the human and mouse cellular receptors for subgroup C adenoviruses and group B coxsackieviruses. Proc. Natl. Acad. Sci. USA **94:**3352–3356.
53. **Von Seggern, D. J., C. Y. Chiu, S. K. Fleck, P. L. Stewart, and G. R. Nemerow.** 1999. A helper-independent adenovirus vector with E1, E3, and fiber deleted: structure and infectivity of fiberless particles. J. Virol. **73:**1601–1608.
54. **Von Seggern, D. J., S. Huang, S. K. Fleck, S. C. Stevenson, and G. R. Nemerow.** 2000. Adenovirus vector pseudotyping in fiber-expressing cell lines: improved transduction of Epstein-Barr virus-transformed B cells. J. Virol. **74:**354–362.
55. **Wickham, T. J.** 2000. Targeting adenovirus. Gene Ther. **7:**110–114.
56. **Wickham, T. J., E. J. Filardo, D. A. Cheresh, and G. R. Nemerow.** 1994. Integrin alpha v beta 5 selectively promotes adenovirus mediated cell membrane permeabilization. J. Cell Biol. **127:**257–264.
57. **Wickham, T. J., P. Mathias, D. A. Cheresh, and G. R. Nemerow.** 1993. Integrins $\alpha_v\beta_3$ and $\alpha_v\beta_5$ promote adenovirus internalization but not virus attachment. Cell **73:**309–319.
58. **Wisnivesky, J. P., P. L. Leopold, and R. G. Crystal.** 1999. Specific binding of the adenovirus capsid to the nuclear envelope. Hum. Gene Ther. **10:**2187–2195.
59. **Yamashiro, D. J., B. Tycko, S. R. Fluss, and F. R. Maxfield.** 1984. Segregation of transferrin to a mildly acidic (pH 6.5) para-Golgi compartment in the recycling pathway. Cell **37:**789–800.